The 9th European Congress on Computational Methods in Applied Sciences and Engineering
ECCOMAS Congress 2024
3–7 June 2024, Lisboa, Portugal

# FLUID-STRUCTURE INTERACTION ANALYSIS OF ASCENDING THORACIC AORTIC ANEURYSMS: A COMPARISON OF PRESTRESSING ALGORITHMS

**ANDRÉ MOURATO[1,2], RODRIGO VALENTE[1,2], MOISÉS BRITO[1,2], JOSÉ XAVIER[1,2], STÉPHANE AVRIL[3], ANTÓNIO C. TOMÁS[4], and JOSÉ FRAGATA[4,5]**

[1] UNIDEMI, Department of Mechanical and Industrial Engineering
NOVA School of Science and Technology, Universidade NOVA de Lisboa
Campus da Caparica, 2829-516 Caparica, Portugal
email: af.mourato@campus.fct.unl.pt, rb.valente@campus.fct.unl.pt,moisesbrito@fct.unl.pt, jmc.xavier@fct.unl.pt

[2] Intelligent Systems Associate Laboratory
Campus Azurém, Guimarães 4800-058,Portugal

[3] École des Mines de Saint-Étienne, University of Lyon
Inserm, Sainbiose U1059, F-42023 Saint-Etienne, France
email: avril@emse.fr

[4] Department of Cardiothoracic Surgery Santa Marta Hospital
Rua de Santa Marta 50, 1169-024 Lisboa, Portugal
email: acruztomas@gmail.com

[5] Department of Surgery and Human Morphology
NOVA Medical School, Universidade NOVA de Lisboa
Campo Mártires da Pátria 130, 1169-056 Lisboa, Portugal
email: jose.fragata@nms.unl.pt

**Key words:** Ascending Thoracic Aortic Aneurysm, Fluid-Structure Interaction, Prestress Tensor, Stress-Free Configuration, Zero Pressure Geometry

**Summary.** Advanced computational techniques, such as Fluid-Structure Interaction (FSI), to model Ascending thoracic Aortic Aneurysms (ATAA) may revolutionize the way precise medicine is performed. One major issue in modelling ATAA biomechanics is the need for the stress-free configuration which is unavailable from imaging data. The Zero Pressure Geometry (ZPG) and Prestress Tensor (PT) are the two main approaches to overcome this issue. However, their impact on the numerical results is yet to be analysed. In this work, three distinct tissue prestressing methodologies were employed and their impact on the numerical results was analysed. The selected tissue prestressing approaches were: (i) ZPG, (ii) PT and (iii) a combination of the PT algorithm with a regional mapping of calibrated material properties (PTCALIB). The results suggested that PT based approaches presented a close agreement with ZPG regarding ATAA hemodynamics. The PT model presented a significantly stiffer mechanical response than the ZPG model. The inclusion of a regional mapping of calibrated material properties contributed

significantly to reduce these differences. Additionally, it was evident that PT based approaches contributed to significantly reduce the amount of iterations required to achieve cycle-to-cycle convergence.

## 1 INTRODUCTION

The field of cardiovascular biomechanics has shown remarkable progress in its ability to develop Ascending Thoracic Aortic Aneurysm (ATAA) digital twins [1]. Although current clinical guidelines recommend surgery for patients with a maximum aortic diameter greater than 55 mm [2], this threshold does not account for individual variability, as some patients with smaller diameters may still experience acute complications, such as rupture or dissection. There is a need for improved risk stratification tools and numerical models that can recreate patient-specific hemodynamics and wall mechanics are a potential tool to accomplish this. Fluid-Structure Interaction (FSI) is the gold-standard methodology for simulating the interaction between hemodynamics and aortic wall mechanics [3–6]. Notwithstanding, the high computational requirements limit its clinical application [7, 8]. Creating FSI models of ATAA requires addressing the challenge of the unavailability of the reference configuration, as the aorta is continuously loaded during the cardiac cycle. Two main tissue prestressing methodologies have been developed to overcome this: Zero Pressure Geometry (ZPG) and Prestress Tensor (PT). The ZPG approach characterize a set of algorithms (e.g., reverse displacement algorithm, modified updated Lagrangian formulation, and generalized prestressing algorithm) that estimate the stress-free configuration through solving minimization problems [9–11]. The PT approach, proposed by Hsu and Bazilevs [12], is more straightforward to implement and focuses on finding the intramural stress state that balances the diastolic hemodynamic loads.

Despite the shared purpose, these approaches may have a significant impact on ATAA numerical modelling. However, in the literature, the relevance of using ZPG or PT methodologies remains unclear. This paper presents a comprehensive systematic comparative analysis of the impact of using different tissue prestressing algorithms on the numerical results estimated by 2-way FSI models implemented in SimVascular. To achieve this objective the biomechanics of one ATAA patient was simulated considering three distinct tissue prestressing methodology: (i) ZPG, (ii) PT and (iii) a novel suggested approach coupling the PT algorithm and a regional mapping of calibrated material properties (PTCALIB). The impact of the prestressing algorithms was evaluated on the pressure field, Wall Shear Stress (WSS) and maximum principal strain and stress due to the relevance of these metrics on the development and progress of cardiovascular disease and estimation of rupture risk.

## 2 MATERIALS AND METHODS

The development of the 2-way FSI models was assisted by patient-specific Computed Tomography Angiography (CTA) and 4D flow Magnetic Resonance Imaging (MRI) data. These data were obtained from a 48-year-old female patient with ATAA and a bovine aortic arch. The medical imaging exams were performed following the research protocol approved by the review board of the *Unidade Local de Saúde São José* and with patient's written informed consent.

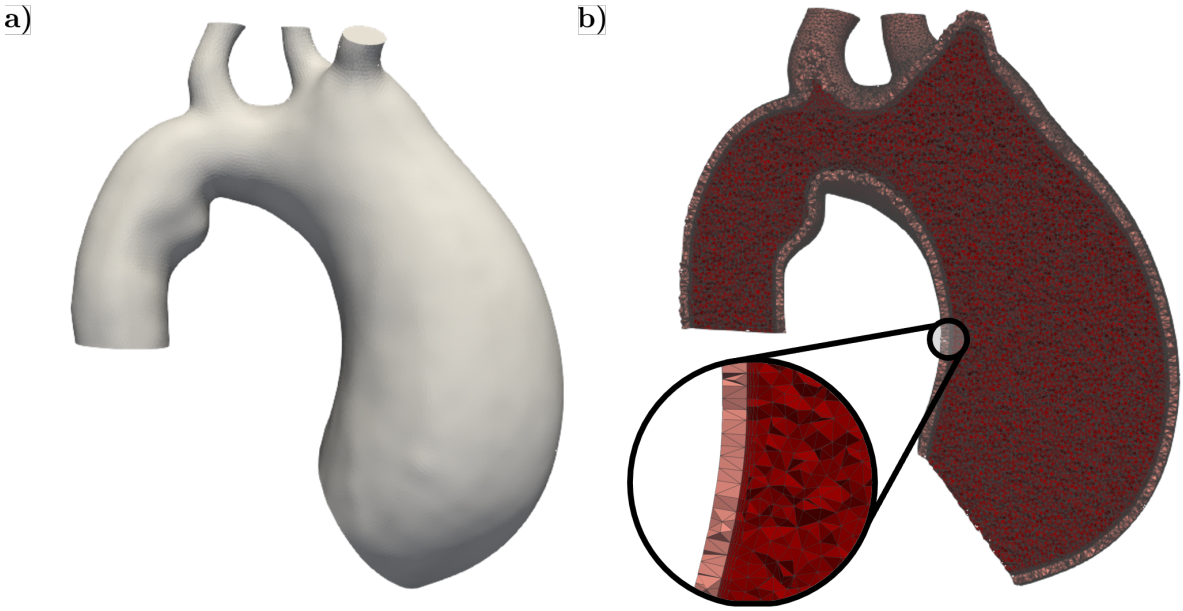


**Figure 1**: Computational domain: **a)** Final lumen virtualization and **b)** representative finite element mesh of the fluid and solid domains.

### 2.1 Segmentation and meshing

The CTA was performed on a revolution CT scanner (GE Healthcare, Milwaukee, WI, USA) and with the administration of iodinated contrast agent (Ultravist 370, Bayer, Leverkusen, Germany). The complete CTA dataset comprised 21 ECG-gated acquisitions. For this work the segmentation was performed at the beginning of the cardiac cycle using the open-source software 3D Slicer [13] which constituted the patient-specific virtualization of the lumen (Fig. 1a). Regarding the virtualization of the aortic wall, as it still remains a challenge the direct extraction from CTA data, a uniform thickness of 1.8 mm was considered. The mesh of both domains (Fig. 1b) was generated, ensuring a nodal correspondence at the interface of the domains, using the Tetgen Libraries tools embedded into SimVascular [14]. The process of mesh generation and mesh sensitivity analysis is described in detail in [15].

### 2.2 Fluid-structure interaction model

Blood can be described as an incompressible solution of plasma and blood cells and exhibits distinctive rheological properties. Nonetheless, in the realm of large arteries hemodynamics the consensus is to model the blood as Newtonian, as well as, the flow as laminar. Fluid viscosity and density are the two only necessary parameters to completely describe the behaviour of a Newtonian fluid and the values used in this work are presented in Table 1.

The aortic wall also exhibits distinctive mechanical behaviour characteristic of an anisotropic, hyperelastic and viscoelastic material. In this work, however, the ATAA wall was modelled as an isotropic, incompressible and Neo-Hookean material [20]. The values chosen for solid domain density and Poisson ratio are also presented in Table 1 and were obtained from the available literature. To find a patient-specific Young Modulus estimation, a simple iterative methodology

**Table 1**: Mechanical properties of the fluid and solid domains.

| Property | Symbol | Units | Value | References |
|---|---|---|---|---|
| Blood density | $\rho_{\mathrm{f}}$ | kg/m$^3$ | 1060 | [16] |
| Viscosity | $\mu$ | Pa.s | $4\times10^{-3}$ | [17] |
| Aortic wall density | $\rho_{\mathrm{s}}$ | kg/m$^3$ | 1120 | [18] |
| Poisson ratio | $\nu_{\mathrm{s}}$ | — | $49\times10^{-2}$ | [19] |

was employed. The volume of the segmentation at 30% of the cardiac cycle was the target value for this calibration process. Computational Solid Mechanics (CSM) simulations considering different Young's Modulus and a pressure boundary condition equivalent to the hemodynamic load at the same instance, were performed until the estimated volume matched the reference value within a margin of error below 5%. The final value of the Young's Modulus was 0.95 MPa.

The interaction between the blood and the aortic wall occurs at the interface between the domains, in which, the hemodynamic loads are transferred to the solid domain and the displacement of the aortic wall updates the fluid domain mesh. SimVascular resorts to a monolithic approach to solve the FSI problem. At the interface, kinematic and dynamic boundary conditions are fulfilled.

$$\boldsymbol{w} = \frac{\partial \boldsymbol{u}}{\partial t} \tag{1}$$

$$\boldsymbol{\sigma}_{\mathrm{f}}\boldsymbol{n}_{\mathrm{f}} + \boldsymbol{\sigma}_{\mathrm{s}}\boldsymbol{n}_{\mathrm{s}} = 0 \tag{2}$$

### 2.3 Boundary conditions

Three different boundary conditions were used to develop the FSI model (Fig. 2). At the fluid domain inlet, a patient-specific flow rate, obtained via MRI, was prescribed and a parabolic velocity profile was assumed. The outlets were coupled with three-element Windkessel models. The patient-specific coefficients (Table 2) were calibrated, using reduced order models implemented in SimVascular, to fit a diastolic systolic pressure variation of 80-120 mmHg. The extremities of the solid domain were fixed not allowing out of plane displacements.

**Table 2**: Patient-specific three-element windkessel models parameters: resistance of larger caliber arteries, $\mathrm{R}_p$, artery compliance, C, and Resistance of smaller arteries and arterioles, $\mathrm{R}_d$.

| Model Parameter | Units | Descending aorta | Brachiocephalic trunk | Left common carotid | Left subclavian |
|---|---|---|---|---|---|
| $\mathrm{R}_p$ | MPa.s.m$^{-3}$ | 15 | 50 | 90 | 70 |
| C | $10^6$ m$^3$.Pa$^{-1}$ | 40 | 7 | 6 | 10 |
| $\mathrm{R}_d$ | MPa.s.m$^{-3}$ | 300 | 850 | 2000 | 1700 |

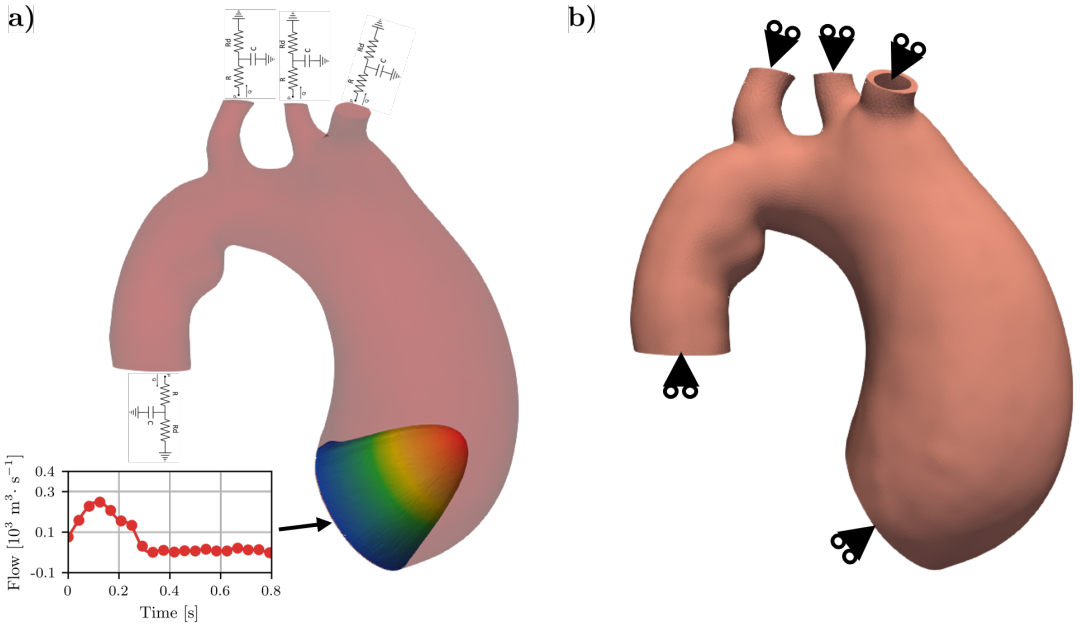


**Figure 2**: Boundary conditions of the fluid and solid domain: **a)** patient-specific flow rate at the inlet; three-element Windkessel models at the outlets and **b)** domain extremities are fixed in the normal direction to the plane.

### 2.4 Tissue prestressing methodologies

The ATAA is constantly loaded during the cardiac cycle by blood pressure and viscous forces. Therefore, the image configuration available in CTA data does not match the reference configuration. This negatively impacts the accuracy of the numerical results, mainly due to the non-linear elasticity of the aortic wall. The two main methodologies to address this issue are the ZPG [9–11] and PT [12, 21]. In this work, a novel method that couples the PT approach and a regional mapping of calibrated of the material properties is also proposed and analysed.

#### 2.4.1 Reverse displacement algorithm

A wide range of methods based on the ZPG approach are available in the literature. In this work, the reverse displacement algorithm proposed by Raghavan *et al.* [9] in 2006 was implemented. The main principle is to estimate a parameter, k, that describes the motion between the reference and image configurations. This parameter is calculated by solving a minimization problem of a distance score which quantifies the differences amidst the deformed candidate configuration (the results of applying the diastolic pressure field on a candidate reference configuration) and the image configuration. The complete description of the reverse displacement algorithm is provided by Raghavan *et al.* [9].

#### 2.4.2 Prestress tensor

The PT methodology was proposed by Hsu and Bazilevs [12] in 2011 and accounts for the diastolic stress state by suggesting a slight modification to the solid domain formulation, propos-

ing to incorporate the PT using the additive decomposition of the second Piola-Kirchhoff stress tensor. This tensor is calibrated in order to balance the diastolic hemodynamic loads applied at the fluid-solid interface. The numerical implementation of this methodology is described in [12].

### 2.4.3 Prestress tensor with calibrated material properties

Previous analyses conducted by our research group revealed that models employing the PT method exhibit a significantly stiffer structural response when compared to those using ZPG algorithms. This phenomenon arises, as depicted in Fig. 3a, due to ZPG algorithms accounting with the (pre)deformation between the reference and image configurations, while the PT approach does not. The PTCALIB method was designed to improve this agreement by suggesting that, after employing the PT algorithm, a regional mapping of calibrated material properties should also be provided when performing structural analysis of the ATAA wall.

The implementation of the PTCALIB methodology involves two main tasks: (i) dividing the ATAA wall mesh into subdomains (Fig. 3b) and (ii) assigning each subdomain a Young's Modulus representative of the stress-strain state at the beginning of the cardiac cycle (Fig. 3c). The following steps were performed to complete these tasks:

1. Create 10 subdomains, $\Omega_{\mathrm{s}}^{j}$.

   (a) Use the estimated PT to calculate the principal stresses average, $\overline{\boldsymbol{\sigma}_{\mathrm{P}}}$, of each element of the solid domain;

   (b) Divide the range of $\overline{\boldsymbol{\sigma}_{\mathrm{P}}}$ into 10 equally spaced intervals. Each of the intervals define a subdomain, $\Omega_{\mathrm{s}}^{j}$. These subdomains follow: $\bigcup_{j=1}^{10} \Omega_{\mathrm{s}}^{j} = \Omega_{\mathrm{s}}^{0}$ and $\bigcap_{j=1}^{10} \Omega_{\mathrm{s}}^{j} = \varnothing$. Additionally, they are characterized by the medium value of principal stresses average, $\overline{\boldsymbol{\sigma}_{\mathrm{P}}}^{j}$.

2. Estimate the new Young's Modulus [22], $E_{\mathrm{Calib}}^{j}$, for each subdomain.

   (a) Virtualize an uniaxial tensile test on a sample of ATAA tissue (considering the Young's Modulus used for the PT) to estimate the relation between the force, $F$, and the stretch, $\lambda$, relative to the deformation between the reference and image configurations;

   (b) Calculate the Kirchhoff stress, $\sigma'$, and Green-St. Venant strain, $\varepsilon'$, as follows:

   $$\sigma' = \frac{F}{A_0 \cdot \lambda} \quad \varepsilon' = \frac{\lambda^2 - 1}{2} \tag{3}$$

   Where $A_0$ is the initial cross-sectional area of the sample;

   (c) Estimate the inverse of the tangent Young's Modulus, $E_T^{-1}$, as the derivative of $\varepsilon'$ with respect to $\sigma'$;

   (d) Attribute the new Young's Modulus, $E_{\mathrm{Calib}}^{j}$, to each subdomain as the estimated tangent Young's Modulus correspondent to $E_{\mathrm{Calib}}^{j} = E_T(\sigma' = \overline{\boldsymbol{\sigma}_{\mathrm{P}}}^{j})$.

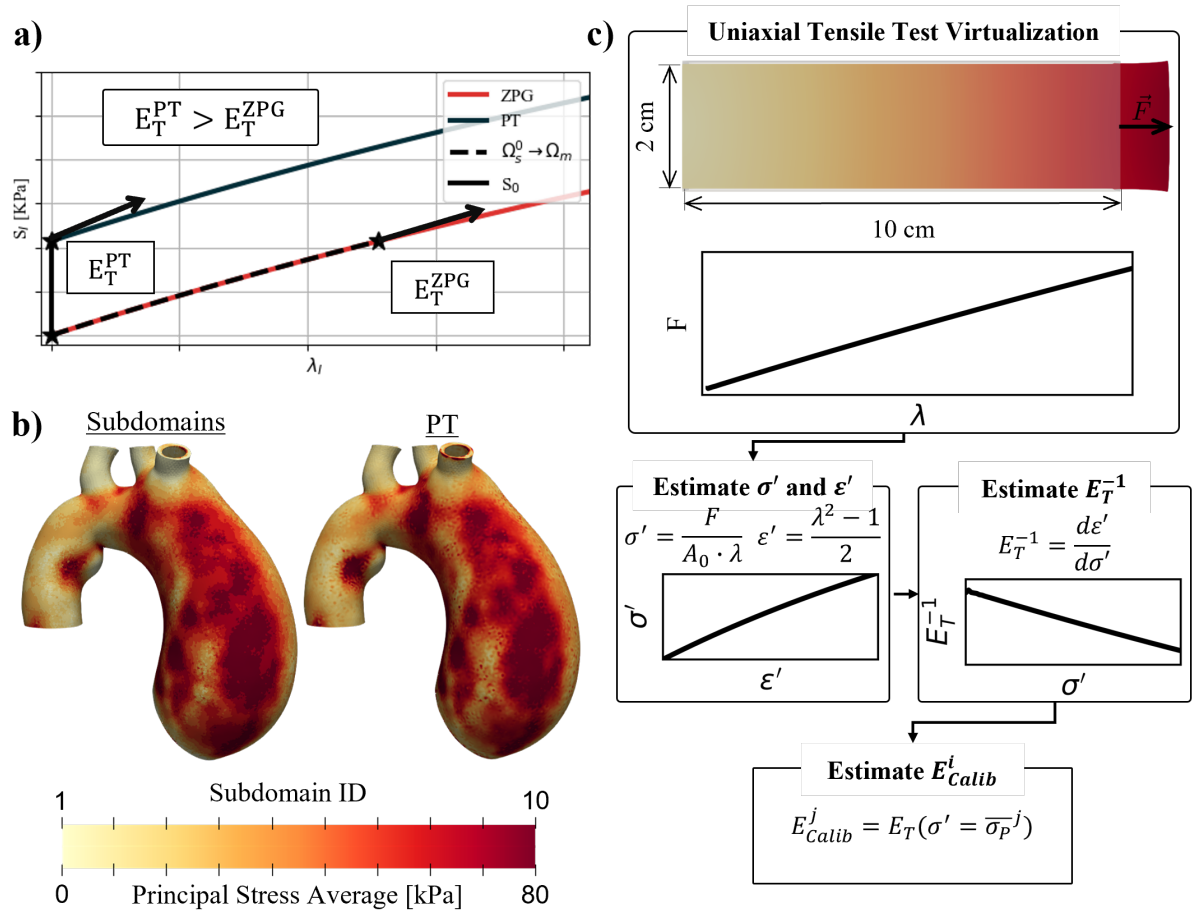


**Figure 3**: **a)** Representative stress-stretch curves of a Neo-Hookean material using the ZPG and the PT approaches; **b)** correspondence between the medium value of Principal Stresses average and **c)** schematic of the numerical implementation of the PTCALIB methodology.

## 3 RESULTS

The impact of different tissue prestressing methodologies on the biomechanical characterization of ATAA using FSI models was measured in this study. Regarding the hemodynamics, both the pressure field and WSS based metrics were analysed due to their positive correlation with the development and progression of aneurysms and the risk of acute complications. The nodal pressure time series of PT and PTCALIB models were compared with the ZPG model using the pairwise Pearson's correlation coefficient, R. Regarding the estimated WSS, the impact was quantified in terms of Time-Averaged Wall Shear Stress (TAWSS) (measures the local average magnitude of WSS) and Oscillatory Shear Index (OSI) (quantifies the directional changes of WSS during the cardiac cycle), which were calculated as follows:

$$\begin{aligned} \text{TAWSS} &= \frac{1}{T}\int_0^T |\text{WSS}|\ dt \\ \text{OSI} &= 0.5\Big(1 - \frac{|\int_0^T \text{WSS}\ dt|}{\int_0^T |\text{WSS}|\ dt}\Big) \end{aligned} \tag{4}$$

To investigate the impact of the prestressing methodologies on the estimated structural response, the maximum principal strain and maximum principal stress were analysed as these are also relevant metrics for the risk stratification of acute complications. Additionally, the cycle-to-cycle convergence was also evaluated by analysing the required iterations until a periodic steady-state is achieved. The periodic steady-state was considered to be obtained when the relative instantaneous difference of estimated pressure in consequent cycles was below 2.5% throughout the cardiac cycle.

### 3.1 Hemodynamics indices

The violin plot of the Pearson's Correlation coefficient regarding the comparison of nodal pressure time series between the ZPG approach, considered the reference values, the PT and PTCALIB models is presented in Fig. 4. The PT based approaches exhibited a strong correlation with the estimated pressure field by the ZPG model (at least 98% of the R values are above 0.99). The violin plots regarding WSS based metrics (Fig. 4), revealed that all models produced similar distributions and average behaviours which is indicative of a good agreement between the ZPG approach, PT and PTCALIB models.

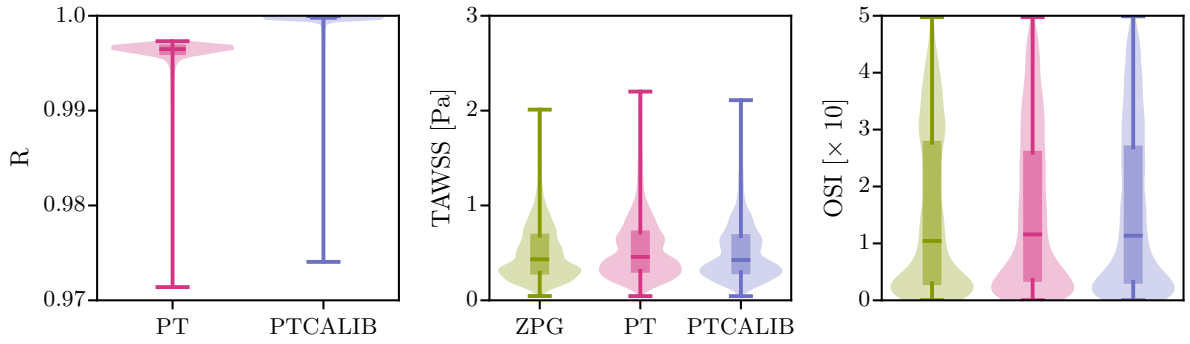


**Figure 4**: Impact of different tissue prestressing methodologies on the ATAA hemodynamics: violin plots of the Pearson's correlation coefficient, TAWSS and OSI.

### 3.2 Structural indices

The impact of different tissue prestressing methodologies on the estimated probability density function of the maximum principal strain and stress in the ATAA wall is presented in Fig. 5. The PT model, as expected, presented a significantly stiffer mechanical response than the ZPG model. The PTCALIB model, outperformed its counterpart, presenting a significantly closer agreement with the ZPG model.

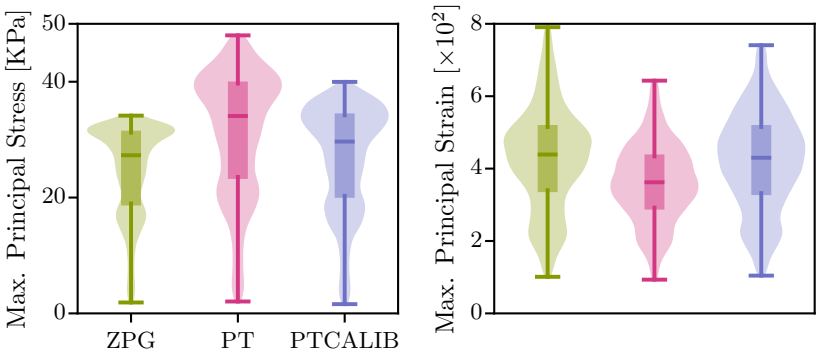


**Figure 5**: Impact of different tissue prestressing methodologies on the ATAA hemodynamics: violin plots of the maximum principal strains and stresses.

### 3.3 Cycle-to-cycle convergence

In Fig. 6 is presented the evolution of the average pressure and the periodic state criterium in three distinct orthogonal slices located along the computational domain (mid ascending aorta, aortic arch and descending aorta). These results show that the PT based algorithms required around 60% fewer iterations to achieve a periodic steady-state than the ZPG models.

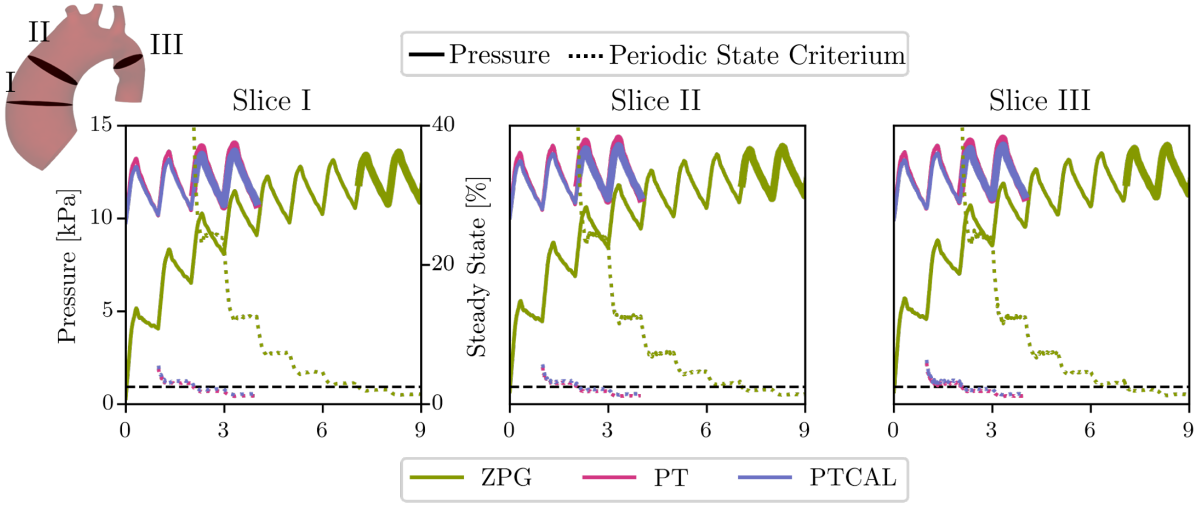


**Figure 6**: Impact of different tissue prestressing methodologies on the cycle-to-cycle convergence: time series of the average pressure and periodic state criterium in three orthogonal slices (mid ascending aorta, aortic arch and descending aorta).

## 4 DISCUSSION

The characterization of the reference configuration is a fundamental step to effectively perform numerical analysis of structures. This poses a concrete problem in modelling the mechanical behaviour of the ATAA wall, as this configuration is not available in imaging data. The ZPG

approach is the most commonly used methodology to estimate the reference configuration and is considered the gold-standard. However, this approach is computationally expensive and complex to implement. In this context, the PT approach emerges as a more straightforward and numerically efficient method.

The results of this study revealed that the PT model produced similar results to ZPG in terms of the estimated ATAA hemodynamics. The estimated structural indices, however, were significantly different as the PT model presented a stiffer mechanical response. The PTCALIB was developed to surpass this limitation. The regional mapping of calibrated material properties aimed to better characterize the stress-strain state at the diastole in order to provide an improved agreement with the ZPG model. The PTCALIB model produced results with equivalent degree of accuracy when compared to PT regarding blood pressure and WSS. However, outperformed the PT model in the estimation of structural indices, presenting a closer agreement with the ZPG model, in both.

One more relevant aspect when aiming towards the introduction of numerical models into clinical practices is the reporting time which can be directly influenced by the amount of iterations required to achieve cycle-to-cycle convergence. In this matter both the PT and PTCALIB models outperformed the ZPG approach as they required around 60% less iterations to achieve the periodic state.

## 5 CONCLUSIONS

In this work the impact of using different tissue prestressing algorithms on the results of FSI simulations of ATAA was investigated. The ZPG, PT and PTCALIB methodologies were employed and the results regarding the estimated blood pressure, WSS, wall mechanics and cycle-to-cycle convergence were compared. The PT and PTCALIB models presented a good agreement with the ZPG models in terms of hemodynamics and required around 60% less iterations to achieve cycle-to-cycle convergence. Regarding the simulation of the ATAA wall mechanics, the PT methodology revealed to produce a stiffer mechanical response than the model using the ZPG approach. The PTCALIB methodology, developed to surpass this issue, outperformed the PT model, presenting a significantly closer agreement with ZPG. This aspect highlights the need to consider a regional mapping of material properties when using the PT approach.

## ACKNOWLEDGMENTS

This research was funded by the Portuguese Foundation for Science and Technology (FCT,IP) under the projects: “Fluid-structure interaction for functional assessment of ascending aortic aneurysms: a biomechanical-based approach toward clinical practice” (AneurysmTool) DOI: 10.54499/PTDC/EMD-EMD/1230/2021; UNIDEMI: UIDB/00667/2020 and UIDP/00667/2020; A. Mourato Ph.D. grant DOI:10.54499/UI/BD/151212/2021, R. Valente Ph.D. grant 2022.12223.BD.

## References

[1] Xuehuan He, Stéphane Avril, and Jia Lu. Prediction of local strength of ascending thoracic aortic aneurysms. *J. Mech. Behav. Biomed. Mater.*, 115:104–284, March 2021.

[2] Raimund Erbel, Victor Aboyans, Catherine Boileau, Eduardo Bossone, Roberto Di Bartolomeo, Holger Eggebrecht, Arturo Evangelista, Volkmar Falk, Herbert Frank, et al. 2014

ESC guidelines on the diagnosis and treatment of aortic diseases: document covering acute and chronic aortic diseases of the thoracic and abdominal aorta of the adult the task force for the diagnosis and treatment of aortic diseases of the European Society of Cardiology (ESC). *Eur. Heart J.*, 35(41):2873–2926, 2014. doi: 10.1093/eurheartj/ehu281.

[3] Rossella Campobasso, Francesca Condemi, Magalie Viallon, Pierre Croisille, Salvatore Campisi, and Stéphane Avril. Evaluation of peak wall stress in an ascending thoracic aortic aneurysm using FSI simulations: effects of aortic stiffness and peripheral resistance. *Cardiovasc. Eng. Technol.*, 9(4):707–722, 2018. doi: 10.1007/s13239-018-00385-z.

[4] André Mourato, Rodrigo Valente, Moisés Brito, José Xavier, António Tomás, Stéphane Avril, José Sá, and José Fragata. Computational modelling and simulation of fluid structure interaction in aortic aneurysms: a systematic review and discussion of the clinical potential. *Appl. Sci.*, 2(2):0–38204, August 2022. doi: 10.3390/app12168049.

[5] Alessandro Mariotti, Alessandro Boccadifuoco, Simona Celi, and Maria V. Salvetti. Hemodynamics and stresses in numerical simulations of the thoracic aorta: Stochastic sensitivity analysis to inlet flow-rate waveform. *Comput. Fluids*, 230:173–182, 2021. doi: 10.1016/j.compfluid.2021.105123.

[6] Marcin Nowak, Bartlomiej Melka, Marek Rojczyk, Maria Gracka, Andrzej J. Nowak, Adam Golda, Wojciech P. Adamczyk, Benjamin Isaac, Ryszard A. Białecki, and Ziemowit Ostrowski. The protocol for using elastic wall model in modeling blood flow within human artery. *Eur. J. Mech. B. Fluids*, 77:273–280, 2019. doi: 10.1016/j.euromechflu.2019.03.009.

[7] Vincent Mendez, Marzio Di Giuseppe, and Salvatore Pasta. Comparison of hemodynamic and structural indices of ascending thoracic aortic aneurysm as predicted by 2-way FSI, CFD rigid wall simulation and patient-specific displacement-based FEA. *Comput. Biol. Med.*, 100:221–229, 2018. doi: 10.1016/j.compbiomed.2018.07.013.

[8] Alvaro Valencia, Patricio Burdiles, Miguel Ignat, Jorge Mura, Eduardo Bravo, Rodrigo Rivera, and Juan Sordo. Fluid structural analysis of human cerebral aneurysm using their own wall mechanical properties. *Comput. Math. Methods Med.*, 2013(1):293128, 2013. doi: 10.1155/2013/293128.

[9] Madhavan L. Raghavan, Baoshun Ma, and Mark F. Fillinger. Non-invasive determination of zero-pressure geometry of arterial aneurysms. *Ann. Biomed. Eng.*, 34:1414–1419, July 2006. doi: 10.1007/s10439-006-9115-7.

[10] Michael W. Gee, Ch Förster, and Wolfgang A. Wall. A computational strategy for prestressing patient-specific biomechanical problems under finite deformation. *Int. J. Numer. Method. Biomed. Eng.*, 26(1):52–72, June 2010. doi: 10.1002/cnm.1236.

[11] Hannah Weisbecker, David M. Pierce, and Gerhard A. Holzapfel. A generalized prestressing algorithm for finite element simulations of preloaded geometries with application to the aorta. *Int. J. Numer. Method. Biomed. Eng.*, 30(9):857–872, March 2014. doi: 10.1002/cnm.2632.

[12] Ming-Chen Hsu and Yuri Bazilevs. Blood vessel tissue prestress modeling for vascular fluid–structure interaction simulation. 47(6):593–599. doi: 10.1016/j.finel.2010.12.015.

[13] Ron Kikinis, Steve D. Pieper, and Kirby G. Vosburgh. 3D slicer: a platform for subject-specific image analysis, visualization, and clinical support. In *Intraoperative imaging and image-guided therapy*, pages 277–289. Springer, 2013.

[14] Adam Updegrove, Nathan M. Wilson, Jameson Merkow, Hongzhi Lan, Alison L. Marsden, and Shawn C. Shadden. Simvascular: an open source pipeline for cardiovascular simulation. *Ann. Biomed. Eng.*, 45:525–541, December 2017. doi: 10.1007/s10439-016-1762-8.

[15] Rodrigo Valente, André Mourato, Moisés Brito, José Xavier, António Tomás, and Stéphane Avril. Fluid-structure interaction modeling of ascending thoracic aortic aneurysms in simvascular. *Biomechanics*, 2(2):189–204, 2022. doi: 10.3390/biomechanics2020016.

[16] Sabrina Ahmed, Desmond Dillon-Murphy, and C. Alberto Figueroa. Computational study of anatomical risk factors in idealized models of type b aortic dissection. *Eur. J. Vasc. Endovasc. Surg.*, 52(6):736–745, 2016. doi: 10.1016/j.ejvs.2016.07.025.

[17] Mir-Hossein Moosavi, Nasser Fatouraee, Hamid Katoozian, Ali Pashaei, Oscar Camara, and Alejandro F. Frangi. Numerical simulation of blood flow in the left ventricle and aortic sinus using magnetic resonance imaging and computational fluid dynamics. *Comput. Methods Biomech. Biomed. Eng.*, 17(7):740–749, 2014. doi: 10.1080/10255842.2012.715638.

[18] Seyed H. Attaran, Hanieh Niroomand-oscuii, and Farzan Ghalichi. A novel, simple 3D/2D outflow boundary model for blood flow simulations in compliant arteries. *Comput. Fluids*, 174:229–240, 2018. doi: 10.1016/j.compfluid.2018.08.006.

[19] Solmaz Farzaneh, Olfa Trabelsi, and Stéphane Avril. Inverse identification of local stiffness across ascending thoracic aortic aneurysms. *Biomech. Model. Mechanobiol.*, 18(1):137–153, 2019. doi: 10.1007/s10237-018-1073-0.

[20] Marwa Selmi, Hafedh Belmabrouk, and Abdullah Bajahzar. Numerical study of the blood flow in a deformable human aorta. *Appl. Sci.*, 9(6):1216, February 2019. doi: 10.3390/app9061216.

[21] Kathrin Bäumler, Vijay Vedula, Anna M. Sailer, Jongmin Seo, Peter Chiu, Gabriel Mistelbauer, Frandics P. Chan, Michael P. Fischbein, Alison L. Marsden, and Dominik Fleischmann. Fluid–structure interaction simulations of patient-specific aortic dissection. *Biomech. Model. Mechanobiol.*, 19(5):1607–1628, 2020. doi: 10.1007/s10237-020-01294-8.

[22] Dimitrios P. Sokolis. Passive mechanical properties and structure of the aorta: segmental analysis. *Acta Physiol.*, 190(4):277–289, January 2007. doi: 10.1111/j.1748-1716.2006.01661.x.